Oecologia (2001) 126:487–499
DOI 10.1007/s004420000543

Elke Naumburg · David S. Ellsworth
Gabriel G. Katul

Modeling dynamic understory photosynthesis of contrasting species in ambient and elevated carbon dioxide

Received: 14 April 2000 / Accepted: 11 September 2000 / Published online: 9 December 2000

Abstract Dynamic responses of understory plants to sunflecks have been extensively studied, but how much differences in dynamic light responses affect daily photosynthesis (A_{day}) is still the subject of active research. Recent models of dynamic photosynthesis have provided a quantitative tool that allows the critical assessment of the importance of these sunfleck responses on A_{day}. Here we used a dynamic photosynthesis model to assess differences in four species that were growing in ambient and elevated CO_2. We hypothesized that *Liriodendron tulipifera*, a species with rapid photosynthetic induction gain and slow induction loss, would have the least limitations to sunfleck photosynthesis relative to the other three species (*Acer rubrum*, *Cornus florida*, *Liquidambar styraciflua*). As a consequence, *L. tulipifera* should have the highest A_{day} in an understory environment, despite being the least shade tolerant of the species tested. We further hypothesized that daily photosynthetic enhancement by elevated CO_2 would differ from enhancement levels observed during light-saturated, steady-state measurements. Both hypotheses were supported by the model results under conditions of low daily photosynthetic photon flux density (PFD; <3% of the above-canopy PFD). However, under moderate PFD (10–20% of the above-canopy PFD), differences in dynamic sunfleck responses had no direct impact on A_{day} for any of the species, since stomatal and photosynthetic induction limitations to sunfleck photosynthesis were small. Thus, the relative species ranking in A_{day} under moderate PFD closely matched their rankings in steady-state measurements of light-saturated photosynthesis. Similarly, under elevated CO_2, enhancement of modeled A_{day} over A_{day} at ambient CO_2 matched the enhancement measured under light saturation. Thus, the effects of species-specific differences in dynamic sunfleck responses, and differences in elevated CO_2 responses of daily photosynthesis, are most important in marginal light environments.

Keywords Daily photosynthesis · Sunflecks · Shade tolerance · Elevated carbon dioxide · Photosynthetic enhancement

E. Naumburg (✉)
Desert Research Institute, 755 E Flamingo Rd,
Las Vegas, NV 89119, USA
e-mail: elke@dri.edu
Tel.: +1-702-8950481, Fax: +1-702-8950427

E. Naumburg · D.S. Ellsworth · G.G. Katul
Nicholas School of the Environment, Duke University,
Durham, NC 27708-0328, USA

D.S. Ellsworth
Department of Enviromental Sciences Brookhaven
National Laboratory, Upton, NY 11973-5000, USA

Introduction

Numerous studies have described the dynamic gas exchange responses of plant species to changes in light intensity (reviewed in Pearcy 1990; Naumburg and Ellsworth 2000). Based on these studies, it is clear that plants can differ in their dynamic responses to light as a function of the local light environment and species-specific characteristics. That is, plants differ in the rate with which they open stomata and activate photosynthetic enzymes in response to high-intensity light during sunflecks, and the rate with which these revert to the initial states in shade. Since these dynamic responses partially determine how well a plant can utilize sunflecks for photosynthesis (Pearcy et al. 1994; Valladares et al. 1997; Naumburg and Ellsworth 2000), the contribution of sunflecks to daily photosynthesis (A_{day}) among plants and species should vary greatly. Indeed, estimates of sunfleck photosynthesis range between 20–80% of A_{day} (Gross 1982; Pearcy and Calkin 1983; Pearcy 1987; Chazdon 1988; Pfitsch and Pearcy 1989) and 9–44% of the annual C gain (Pearcy and Pfitsch 1991). However, it is unclear how much of these differences in sunfleck contribution to photosynthesis are due to differences in light regimes rather than species-specific differences in dynamic light responses or photosynthetic capacity. To date, a link between differences in dynamic photosynthetic light responses among species and distinct differences in daily C

uptake in the field is lacking. However, indirect evidence of such a link can be found in growth studies that show species differences in biomass responses to homogeneous versus variable light (Sims and Pearcy 1993; Wayne and Bazzaz 1993; Watling et al. 1997).

The difficulty in quantifying the importance of dynamic light responses is related to the transient nature of sunflecks in the understory. In a natural ecosystem, each leaf grows in a unique sunfleck light environment with different daily totals in photosynthetic photon flux density (PFD) Further, distributions of sunflecks vs. shade periods vary with weather conditions such as cloud cover and wind and seasonal changes in sun angle and canopy leaf area (Chazdon 1988; Pearcy et al. 1996). Consequently, daily measurements of gas exchange are of limited use in comparative studies since no two leaves experience the same light regime. As an alternative, models (e.g., Pearcy et al. 1994), can be used to determine the significance of sunflecks and dynamic photosynthetic responses, but these have rarely been parameterized and applied to contrasting species in field conditions. In the absence of robust species comparisons in field light environments, the importance of differing dynamic responses on A_{day} is unclear (Pearcy et al. 1996).

Previously, we observed that understory saplings of two shade-tolerant and two intolerant species differed in their dynamic gas exchange responses to lightflecks (Naumburg and Ellsworth 2000). Specifically, *Acer rubrum* L. (red maple) showed rapid induction gain/loss in response to changes in PFD while *Cornus florida* L. (flowering dogwood) and *Liquidambar styraciflua* L. (sweetgum), in particular, were less responsive. *Liriodendron tulipifera* L. (tulip-poplar) showed asymmetrical behavior to changes in PFD in that it gained induction rapidly after increases in PFD and lost induction comparatively slowly after decreases in PFD. This latter behavior would be optimal for utilizing sunflecks efficiently for photosynthesis since, after several sunflecks, it would achieve a high induction state to maintain through subsequent shade periods (Chazdon 1988; Naumburg and Ellsworth 2000). In contrast, species such as *A. rubrum* that lose induction rapidly during shade would experience higher induction limitation to sunfleck photosynthesis than *L. tulipifera*. And finally, species with slow induction gain such as *L. styraciflua* may never reach high induction states in environments were sunflecks are rare and thus, this type of dynamic behavior would also lead to high induction limitation to sunfleck photosynthesis.

Here, we evaluate to what extent the observed species differences in short-term dynamic gas exchange responses affect leaf A_{day} in the understory. We employed the semi-mechanistic sunfleck photosynthesis model of Pearcy et al. (1997) to test the hypothesis that the dynamic response of *L. tulipifera* leads to higher A_{day} and lower induction limitation to sunfleck photosynthesis than the dynamic behavior of the other previously studied species. We used measurements and model parameterizations for understory saplings growing in ambient and elevated atmospheric CO_2 since: (1) we previously (Naumburg and Ellsworth 2000) observed differences in the dynamic responses of photosynthesis to lightflecks between ambient and elevated CO_2-grown saplings, and (2) some studies have suggested that differences in understory species' responses to elevated CO_2 will drive compositional changes in forests in a future, higher CO_2 atmosphere (Bolker et al. 1995; Kerstiens 1998). We tested the hypothesis that CO_2 enhancement ratios of A_{day} differ from those measured using steady-state, instantaneous photosynthesis measurements due to the dynamic nature of photosynthesis and elevated-CO_2-induced changes in dynamic photosynthetic responses to variable light such as slower induction loss under shade (Naumburg and Ellsworth 2000).

Materials and methods

Model

The sunfleck photosynthesis model employs the theory and parameterization equations in Pearcy et al. (1997) and Kirschbaum et al. (1998). Briefly, the model consists of three major modules: (1) an initialization module equilibrating dynamic model variables to the starting PFD value, (2) a dynamic stomatal light response model, and (3) a dynamic photosynthesis model based on the biochemistry of CO_2 fixation. The initialization module generates steady-state solutions for the dynamic model variables based on the initial light value. These values then serve as initial conditions in the dynamic modules of the model. The stomatal module contains four time constants that affect the speed with which stomatal conductance responds to changes in PFD (Kirschbaum et al. 1988; Pearcy et al. 1997). The biochemical module is based on the widely-used Farquhar and von Caemmerer (1982) photosynthesis model but includes time constants for the activation/deactivation of Rubisco and RuBP regeneration enzymes as a function of changes in PFD (Pearcy et al. 1997; Kirschbaum et al. 1998). For completeness, Appendix I summarizes the model equations and integration routines used to solve for A_{net} in our model implementation.

The model was separately parameterized for each of the four species and ambient/elevated CO_2 treatments based on gas exchange responses to controlled changes in light intensity (Naumburg and Ellsworth 2000). The model parameter list with the determination procedure and the range of parameter values are shown in Table 1. Briefly, the model parameterization was based on gas exchange experiments conducted on individual leaves of the study species at the study site (Naumburg and Ellsworth 2000). The time courses of net CO_2 assimilation and stomatal conductance were followed in leaves that were exposed to experimental pulses of saturating light (~1000 μmol m^{-2} s^{-1}), with intervening shade periods (~45 μmol m^{-2} s^{-1}) lasting 2, 6, and 12 min. The measurements were conducted with a CIRAS-1 portable photosynthesis system (PP-Systems, Hitchin, UK) at ~60% relative humidity, 28° C, and the plants' day-time CO_2 concentration. Additional measurements for model parameterization were derived from steady-state measurements of photosynthetic response curves for CO_2 concentrations ≤57.0 Pa (see Naumburg and Ellsworth 2000), and photosynthetic PFD response curves. Further, to verify parameters controlling post-illumination CO_2 fixation, gas exchange measurements were conducted with a Li-Cor 6400 photosynthesis system (Licor, Lincoln, NE) where PFD was varied between shade and saturating PFD at 10 s to 1 min intervals. For each model parameterization, the average responses of plants growing in three separate plots were used. Species- and CO_2-specific values of the time constants controlling the dynamic behavior are listed in Table 2 together with key steady-state parameters.

Table 1 Model parameters used to simulate dynamic photosynthesis in understory light environments, and their range of values for the four study species growing at two growth CO_2 concentrations. Parameters were derived from literature or specified measurements. (*PFD* Photosynthetic photon flux density, A_{net} net photosynthesis)

Symbol	Description	Value or range	Source
Stomatal module			
g_{wsat}	Light-saturated stomatal conductance to water vapor	86-115 mmol m^{-2} s^{-1}	PFD response curve
α_g	Initial slope of g_w light response	0.46-1.09 mol mol^{-1}	PFD response curve
θ_g	Curvature parameter	0.46-0.72	PFD response curve
τ_{gi}	Time constant for biochemical opening signal	32-155 s	Naumburg and Ellsworth (2000); stomatal response to 12-min shade period and subsequent saturating PFD
τ_{gd}	Time constant for biochemical closing signal	90-500 s	Naumburg and Ellsworth (2000); stomatal response to 12-min shade period and subsequent saturating PFD
τ_{gk}	Time constant for osmotica in-/efflux	64-350 s	Naumburg and Ellsworth (2000); stomatal response to 12-min shade period and subsequent saturating PFD
τ_{gw}	Time constant for water in-/efflux	0-277 s	Naumburg and Ellsworth (2000); stomatal response to 12-min shade period and subsequent saturating PFD
Photosynthetic module			
c_a	Atmospheric CO_2 concentration	36.5 or 56.5 Pa	
V_{cmax}	Maximal Rubisco activation in high light	27-43 µmol m^{-2} s^{-1}	CO_2 response curve
V_{cmin}	Minimal Rubisco activation in dark	2.7-4.2 µmol m^{-2} s^{-1}	10% of V_{cmax}; fit low PFD A_{net} in PFD response
α_R	Initial slope of Rubisco activation light response	0.05-0.13 mol mol^{-1}	Fit intermediate PFD A_{net} in PFD response
θ_R	Curvature parameter of Rubisco activation light response	0.70-0.90	Fit intermediate PFD A_{net} in PFD response
τ_{Ri}	Time constant for Rubisco activation in light	70-130 s	Naumburg and Ellsworth (2000); time constant for increase in biochemical induction during initial saturating PFD in controlled light experiments
τ_{Rd}	Time constant for Rubisco deactivation	300-1,200 s	Fit increase in A_{net} after 6- and 12-min shade in controlled light experiment
V_{Fmax}	Maximal RuBP regeneration rate in high PFD	49-75 µmol m^{-2} s^{-1}	1.8×V_{cmax} (Pearcy et al. 1997; Leuning 1995)
V_{Fmin}	Minimal RuBP regeneration rate in dark	0.1 µmol m^{-2} s^{-1}	~0.2% of V_{Fmax} (almost completely deactivated in shade; Sassenrath-Cole and Pearcy 1994)
α_F	Initial slope of RuBP regeneration rate light response	0.3 mol mol^{-1}	Set high to accommodate almost complete activation at light intensities lower than light saturation (Sassenrath-Cole and Pearcy 1994)
θ_F	Curvature parameter of RuBP regeneration rate light response	0.95	Set high (0.95) to accommodate almost complete activation at light intensities lower than light saturation (Sassenrath-Cole and Pearcy 1994)
τ_{Fi}	Time constant for RuBP regeneration activation in light	90 s	Sassenrath-Cole and Pearcy (1994)
τ_{Fd}	Time constant for RuBP regeneration deactivation	180 s	Sassenrath-Cole and Pearcy (1994)
V_{Jmax}	Maximal electron transport in high light	54-84 µmol m^{-2} s^{-1}	2.0×V_{cmax} (Leuning 1995)
α_J	Quantum yield of electron transport	0.07-0.12 mol mol^{-1}	To fit low PFD A_{net} in PFD response curve
θ_J	Curvature parameter of electron transport	0.80-0.95	To fit low PFD A_{net} in PFD response curve
R_{max}	Maximum RuBP pool size	27-42 µmol m^{-2}	1×V_{cmax} to fit post-illumination fixation during fast response measurements
K_R	Apparent Michaelis-Menten constant for RuBP utilization by Rubisco	1 µmol m^{-2}	Fast response measurements, Kirschbaum et al. (1998)
T_{max}	Maximum triose phosphate pool size	13.5-20.8 µmol m^{-2}	~0.5×V_{cmax} to fit post-illumination fixation during fast response measurements
K_T	Apparent Michaelis-Menten constant of RuBP regeneration to triose phosphates	15 µmol m^{-2}	Fast response measurements, Kirschbaum et al. (1998)
r_d	Non-photorespiratory day respiration	0.47-0.62 µmol m^{-2} s^{-1}	PFD response curve
Ψ	Decay rate of glycolate pool intermediates	0.05-0.15 s^{-1}	Fit to observed post-illumination CO_2 burst

Table 1 (continued)

Symbol	Description	Value or range	Source
K_c	Michaelis-Menten constant for carboxylation reaction of Rubisco	31 Pa	Pearcy et al. (1997)
K_o	Michaelis-Menten constant for oxygenation reaction of Rubisco	15,500 Pa	Pearcy et al. (1997)
Γ^*	CO_2 compensation in absence of photorespiration	4.44 Pa	Pearcy et al. (1997)

Table 2 Light-saturated A_{net} (μmol m^{-2} s^{-1}) of the four study species as predicted by the models, V_{cmax} (μmol m^{-2} s^{-1}), g_{wsat} (mmol m^{-2} s^{-1}), and the time constants (τ; s) controlling species-specific dynamic responses in the model. See Table 1 for explanation of the time constants, and other abbreviations

	A_{net}	V_{cmax}	g_{wsat}	τ_{gi}	τ_{gd}	τ_{gk}	τ_{gw}	τ_{Ri}	τ_{Rd}
Ambient CO_2 parameterizations									
A. rubrum	6.6	37	115	155	95	64	64	130	300
C. florida	4.7	27	75	102	195	186	186	120	1000
L. styraciflua	6.4	37	106	51	500	278	277	130	900
L. tulipifera	5.8	31	113	59	401	116	118	105	800
Elevated CO_2 parameterizations									
A. rubrum	10.0	42	95	32	90	165	26	130	500
C. florida	9.9	41	86	97	149	266	113	130	1100
L. styraciflua	10.5	41	130	40	232	256	255	130	1200
L tulipifera	6.9	27	105	66	217	350	0	70	1200

The model can be used to evaluate the effect that different limitations have on instantaneous photosynthesis (A_{net}) and A_{day} estimates by setting individual time constants to zero (Pearcy et al. 1994, 1997). If all time constants are set to zero, the model predicts photosynthesis equivalently to a light response curve (steady-state model).

Study site and data collection

Data for model parameterization, verification and application were collected at the FACTS-1 site in Duke Forest, North Carolina, USA which is equipped with six free-air CO_2 enrichment (FACE) rings described in Hendrey et al. (1999). The site is located in a loblolly pine (*Pinus taeda* L.) plantation established in 1983. Hardwood seedlings and saplings are abundant in the sub-canopy and understory. At the site, three rings are operating at ambient atmospheric [CO_2] and three at ambient +20.0 Pa CO_2 in the pine canopy. At the height of the study saplings in the center of the ring, mean daytime [CO_2] during the 1999 growing season was 56.2±1.8 Pa (mean±1 SD) for n=3 elevated CO_2 rings and ~38.1 Pa in the ambient rings [Hendrey et al. unpublished data; see also Hendrey et al. (1999)]. CO_2 fumigation at the study site began in August 1996.

Model validation

During May and July 1999, daily courses of gas exchange in the study species were measured on plants growing in similar light environments (data not shown) as those used for model parameterization. Conditions in the leaf chamber of the CIRAS-1 photosynthesis system were tracking ambient temperature, humidity, and PFD. Environmental conditions and gas exchange were logged at 5-s intervals. All daily courses were measured on mostly sunny days. In July we measured the full complement of daily gas exchange for 2 trees species^{-1}×2 CO_2 treatment levels×4 species (16 days total). In May, the full complement of measurements was not completed due to the onset of drought, but the data included 2 trees species^{-1} CO_2-treatment^{-1} for *A. rubrum* and *L. tulipifera* and one *C. florida* and two *L. styraciflua* saplings for 11 days in total. Using the PFD data collected for the measurement leaves on these days, daily gas exchange was then modeled at 5-s intervals using the specific species and CO_2-treatment model parameterizations. To evaluate whether the dynamic model performed better than a steady-state model, both the dynamic and steady-state versions of the model parameterizations were run using the daily PFD data and the results compared to measured photosynthesis. Model performance was evaluated using root mean squared differences (RMSE) between the predicted and measured rates of photosynthesis at several time steps. RMSE was defined as:

$$\mathrm{RMSE} = \sqrt{\sum_{i=1}^{N}(A_{pred} - A_{meas})^2}$$

where N=455/t, t is the averaging time interval, 455 is the average time length of the daily measurements in minutes (centered on noon), and A_{pred} and A_{meas} are the predicted and measured A_{net}, respectively. In the understory, the rest of the photoperiod is characterized by low sun angles, and hence sunflecks are negligible, so we focussed our analysis on the 455-min period. We used this analysis of model performance and several time intervals (1, 5, 10, 30, 60, 120, 455 min) over which measured and modeled A_{net} were averaged before calculating RMSE to assess whether model performance was dependent on the length of the time interval of interest.

Deviations from measured A_{net} could be due to both a systematic offset of model predictions during much of the measurement data set or due to failure of the model in reproducing both amplitude and dynamics of understory photosynthesis. The former would likely be due to incorrect steady-state parameters while the latter would be due to either dynamic or steady-state parameters controlling A_{net}. For this reason we repeated the RMSE analysis with the mean daily A_{net} subtracted from both the predicted and

measured A_{net}. This comparison assessed how well the model reproduced the rapid transients and excursions in the measurements.

To evaluate whether the dynamic models predicted A_{net} better than the steady-state models, dynamic RMSE were subtracted from steady-state RMSE. Positive values of this difference RMSE indicate a better fit of the dynamic than the steady-state model.

Light data and model application

PFD measurements were collected at the FACTS-1 site and in an adjacent mature oak-hickory forest. Forest understory PFD was measured using gallium arsenide photodiodes (GA-1118; Hamamatsu, Bridgewater, N.J.) that were calibrated against a commercial quantum sensor reading PFD (LI-190; Li-Cor, Lincoln, Neb.) under a range of shade and sky conditions. Calibrated photodiodes were attached to leaves on understory tree branches 1–2 m above the ground. Twenty-four locations in the pine forest near each of the four species were chosen to represent a range of daily PFD and sunfleck distributions in this forest, which is very close to reaching crown closure (D. Ellsworth, unpublished data). Additionally, photodiodes were positioned at six locations under a closed canopy in the hardwood forest which had similar daily PFD as shady pine sites but more sunflecks with lower average intensity. Data loggers (Campbell 23X; Campbell Scientific, Logan, Utah) read PFD at 0.5-s intervals and recorded 5-s PFD averages for each photodiode over 11 h day^{-1} centered around solar noon. PFD data were collected for 10 days in early June 1999, 6 weeks after leaf emergence for the hardwood trees. From the measurement days, a single day during which sky conditions were sunny and clear was chosen for modeling photosynthesis of each species at ambient and elevated CO_2 using all 30 PFD courses.

Two versions of the model were applied to the PFD data set: the dynamic model with all time constants and the steady-state model with all time constants set to zero. To evaluate the effect different species-specific sunfleck dynamics had on sunfleck photosynthesis, ratios of the dynamic model photosynthesis outputs were calculated relative to the steady-state model outputs.

Statistics

Differences in the RMSE values between steady-state and dynamic model results were analyzed with repeated measures ANOVA. The time-averaging interval (1–455 min) was the repeated factor. CO_2 treatment and species were fixed factors included in the model. To test whether the ambient and elevated CO_2 models differed in how well they described the elevated CO_2 diurnal courses, a similar difference RMSE was calculated and analyzed using the averaging interval and species as fixed factors.

Model predictions of daily photosynthesis at high and low PFD were analyzed by ANOVA because daily PFD appeared to affect the degree to which species dynamic behavior affected A_{day} (see results below). This analysis included daily PFD (two levels) as a fixed factor and CO_2 treatment and species as repeated factors. Both CO_2 and species were considered as repeated factors because the different model parameterizations were all run on the same PFD data and therefore, the model outputs are in essence repeated measures on the same subjects. All analyses were conducted in SAS version 6.12 for Windows (SAS Institute, Cary, N.C.).

Results

Model testing

Although the models were parameterized for an "average" plant using data collected in separate experiments, the dynamic model generally reproduced the dynamic sunfleck responses measured (Fig. 1). Fine-scale features of dynamic photosynthesis in sunflecks in the understory were captured by the dynamic model. The steady-state model also reproduced most features in the measured data generated by sunflecks, but, as expected, it predicted higher peak A_{net} during sunflecks. The differences in peak A_{net} between the dynamic and steady-state models (Fig. 1) indicates limitations to photosynthesis that are mostly attributable to biochemical induction and stomatal opening responses.

We compared performance of the dynamic and steady-state models to determine the utility of the more elaborate, and hence difficult to parameterize, dynamic model. The change in the difference between the steady-state and dynamic RMSE showed that the performance of the two model types became similar with increasing time over which A_{net} was averaged (P=0.01, Fig. 2). At time intervals between 1 and 120 min, the RMSE difference differed significantly ($P \leq 0.05$) among the study species. RMSE differences between the two models were comparatively small for *L. styraciflua* and *L. tulipifera* even at short time intervals, whereas RMSE differences were consistently larger for *A. rubrum* (Fig. 2). These results indicate that considering induction limitations to photosynthesis under variable PFD are important at short time scales (≤10 min) irrespective of species-specific sunfleck response dynamics. In addition, for species that have shown high responsiveness to changes in PFD such as *A. rubrum*, these limitations can be important even for the entire day. On the other hand, for species that show dynamic light behavior that should minimize induction limitations (e.g., *L. tulipifera*), differences in model performance appear small over an entire day. RMSE differences of the order of 0.1 μmol CO_2 m^{-2} s^{-1} are small relative to the typical tree-to-tree variance in light-saturated A_{net} in understory trees (SE≥0.7 μmol m^{-2} s^{-1}; Naumburg and Ellsworth 2000; DeLucia and Thomas 2000), but a deviation of predicted from actual values by 0.1 μmol m^{-2} s^{-1} would scale to ca. 4 mmol m^{-2} day^{-1}.

Errors in the dynamic model A_{net} predictions (e.g., RMSE) were not due to a systematic bias of the model predictions. Calculating RMSE after first subtracting the mean daily measured and modeled A_{net} for both measured and modeled A_{net}, yielded similar RMSE as using non-transformed data (data not shown). If there was a systematic bias in the model parameterizations, then we would have expected smaller RMSE of the transformed data. Further, using the same approach on the steady-state model predictions resulted in ~25% larger RMSE differences between the dynamic and steady-state models at 1–10 min than in Fig. 2 because the dynamic model predicted the variability of the measured photosynthesis data better. This analysis further indicates that the dynamic model generally reproduces understory photosynthesis better than the steady-state model.

Since 50–80% of understory leaf A_{day} occurs during sunflecks and leaves are maintained near photosynthetic compensation during diffuse light periods (Fig. 1), model performance was tested for sunfleck periods defined

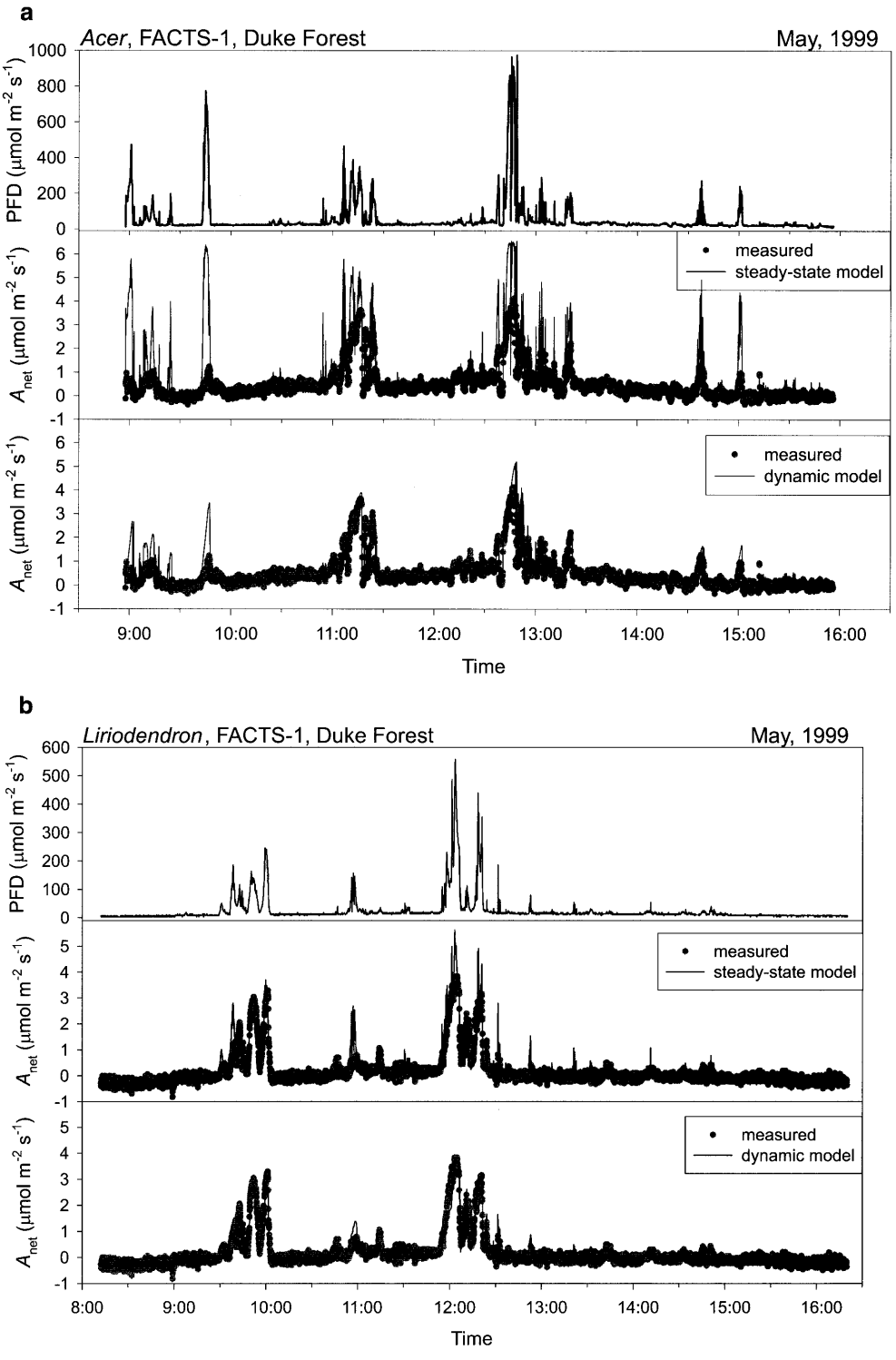

Fig. 1 Daily courses of photosynthesis (A_{net}) for *Acer rubrum* and *Liriodendron tulipifera* collected tracking ambient light, humidity and temperature conditions. *Panels* show the daily course of measured photon flux density (*PFD*), measured A_{net}, and modeled A_{net}. A_{net} was modeled using the PFD recorded during measurements. Two model types were used: a dynamic model where photosynthetic and stomatal induction dynamics are modeled, and a steady-state version of the model where responses to changes in PFD were assumed to be instantaneous

as periods with PFD>100 µmol m^{-2} s^{-1}. The dynamic model more accurately predicts A_{net} during sunflecks than the steady-state model, especially when daily sunfleck A_{net} is low (Fig. 3). When daily sunfleck A_{net} is high and sunflecks are frequent, of long duration and high intensity, the models perform similarly because under such sunfleck regimes limitations to sunfleck photosynthesis are comparatively low. Thus under conditions where sunflecks are infrequent but critical for daily CO_2 assimilation (see Fig. 4 below), the steady-state model has a significant bias suggesting that the dynamic model is more appropriate.

To understand if the intrinsic differences in sunfleck behavior under elevated CO_2 observed by Naumburg and Ellsworth (2000) significantly affect A_{day}, the steady-state and dynamic models were run for elevated CO_2

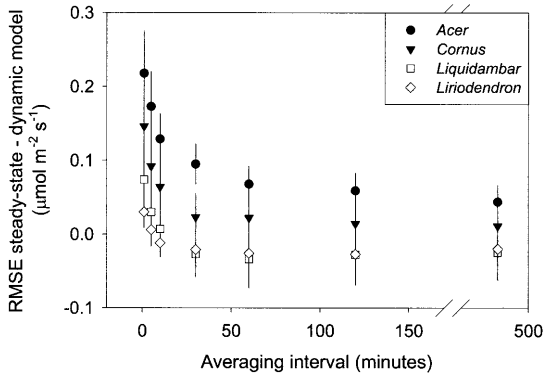

Fig. 2 Difference in root mean squared errors (*RMSE*, a measure of model performance, see Materials and methods) between the steady-state and dynamic model results. Shown are means±1 SE for the four study species averaged for both ambient and elevated CO_2 and time intervals over which both predicted and measured A_{net} were averaged. *Positive values* indicate that the dynamic model predicted measured A_{net} better than the steady-state model

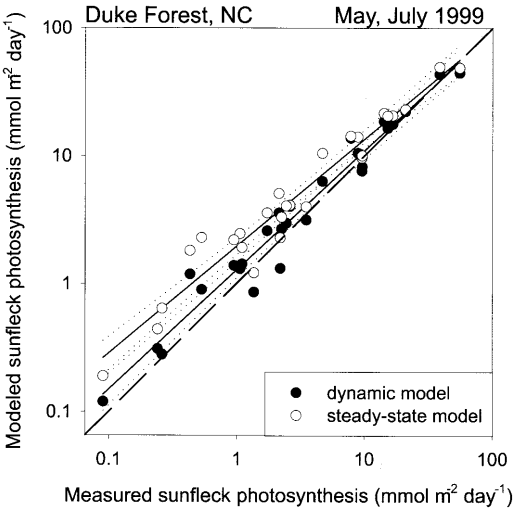

Fig. 3 Comparison between sunfleck photosynthesis (PFD>100 μmol m^{-2} s^{-1}) measured and predicted by the dynamic and steady-state models. The regression equation for the dynamic model estimates is: $\ln(Y)=0.93\times\ln(X)+0.25$, $r^2=0.96$, $P<<0.01$ and for the steady-state model estimates: $\ln(Y)=0.84\times\ln(X)+0.68$, $r^2=0.95$, $P<<0.01$. The slope of the two regressions was marginally significantly different ($P=0.09$), while the intercepts were significantly different ($P<<0.01$). *Dotted lines* around the regressions show the 95% regression confidence intervals while the *dashed line* shows the 1:1 relationship

conditions but with parameters derived under ambient CO_2. These model runs used the same PFD data from the daily measurements of PFD and photosynthesis, which constituted 27 daily measurement cycles. Differences in the RMSE between the two parameterizations were not statistically significant for either species or averaging time interval (data not shown). Further, overall means of the RMSE for ambient parameterizations run at elevated CO_2 vs. elevated CO_2 parameterization were not statistically significantly different ($P>0.1$). This is not surprising because the spatial variability in species parameters is much larger than the effect of CO_2 treatment on the ensemble of physiological variables. Thus, with such variability, either parameterization reproduces A_{day} of the measured elevated CO_2 plants well. To further explore this point, we used three different model parameterizations for predicting elevated CO_2 A_{day} with the dynamic model: (1) the ambient CO_2 parameterizations running at elevated CO_2, (2) the ambient CO_2 parameterizations running at elevated CO_2 with the elevated CO_2 values for maximal Rubisco activation in high light (V_{cmax}) and parameters that scale from V_{cmax} [maximal electron transport in high light (V_{jmax}), maximal RuBP regeneration rate in high PFD (V_{fmax}), maximum triose phosphate pool size (T_{max}), maximum RuBP pool size (R_{max}), Table 1], and (3) the elevated CO_2 parameterizations. In essence, this approach allowed us to conduct a sensitivity analysis determining the impact that observed changes in biochemical kinetics and dynamic parameters can make vis-à-vis absolute differences in photosynthetic rates.

Model application to daily PFD measurements

A_{day} *at ambient* CO_2

Among the 30 photodiodes measuring PFD in the forest understory at the site, daily integrated PFD ranged between 1.0–9.3 mol m^{-2} for the 11 h. This was equivalent

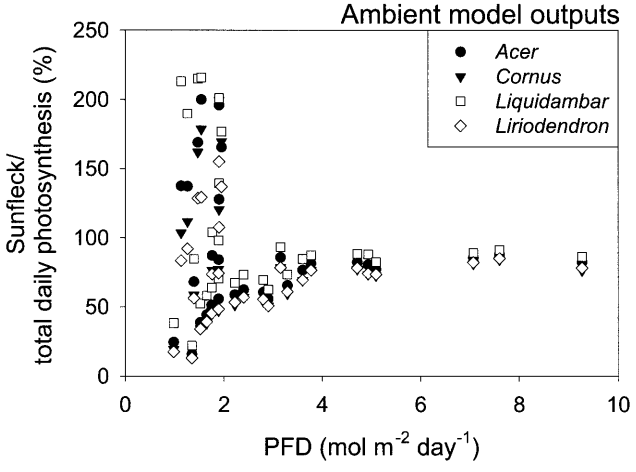

Fig. 4 Ratio (expressed as %) of sunfleck photosynthesis relative to total daily photosynthesis as predicted by the dynamic model for 11-h diurnals. Photosynthesis was modeled using PFD data collected at the study site that had a range of daily PFD and sunfleck characteristics. Shown are the model estimates for ambient CO_2 leaves of the four study species

to 2–17% of the PFD received above the canopy on sunny days. Within the data set, the contribution of sunflecks to daily PFD as well as the number and average intensity of sunflecks combined to give a range of different sunfleck environments (Naumburg and Ellsworth to be published).

The importance of sunflecks (PFD>100 μmol m^{-2} s^{-1}) to A_{day} as predicted by the ambient CO_2 dynamic model is high for clear and sunny days. At daily PFD <2 mol

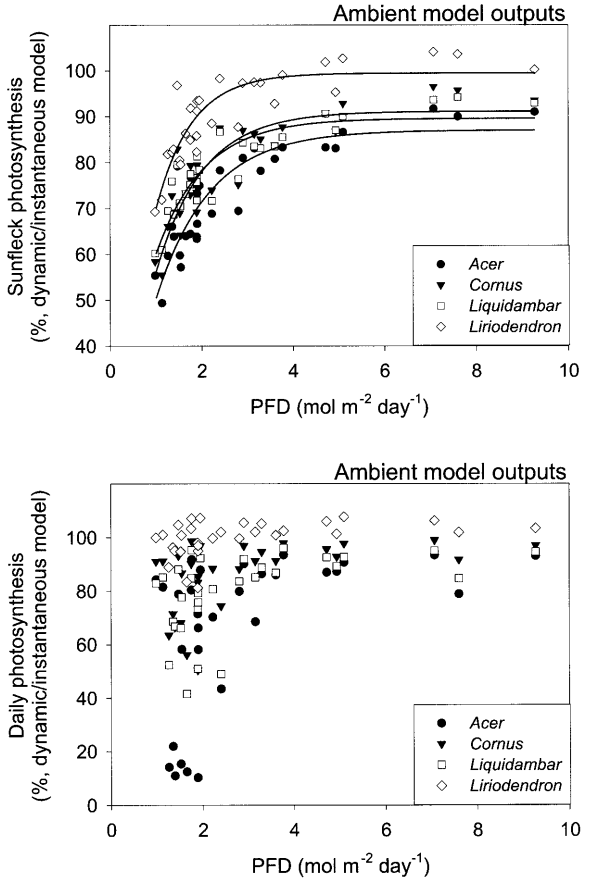

Fig. 5 Ratio of sunfleck and daily photosynthesis predicted by the dynamic model compared to the steady-state model (expressed as %). Data are from model runs for ambient leaves of the study species. Daily photosynthesis can exceed 100% because high induction states after sunflecks increase shade photosynthesis over the steady state value. No regression lines are shown for daily photosynthesis ratios because of the high variability at daily PFD <3 mol m^{-2}

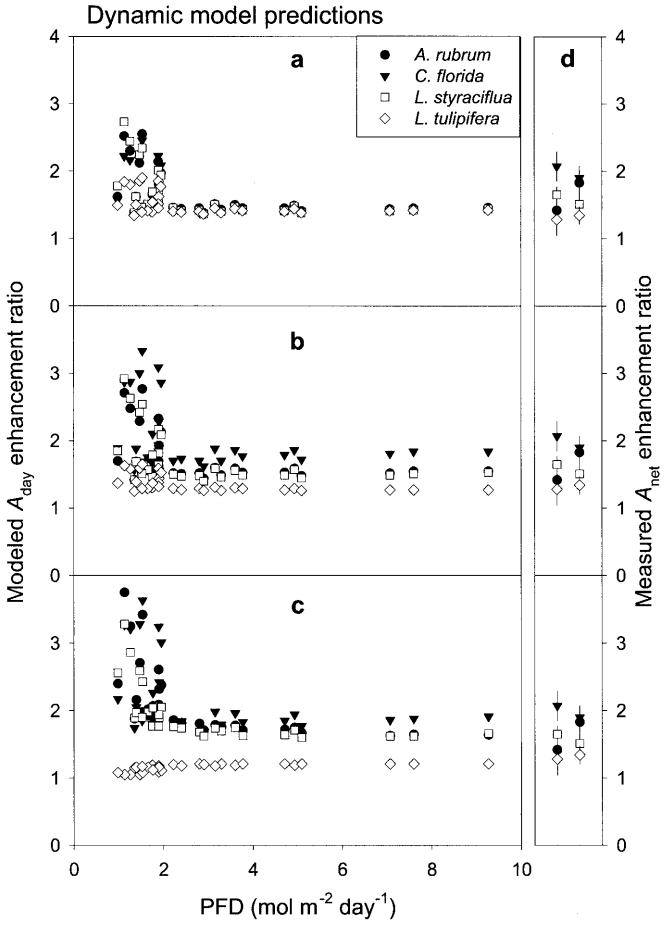

Fig. 6 Enhancement of daily photosynthesis by elevated CO_2 (ratio of elevated/ambient A_{day}) under three modeling scenarios: **a** ambient model parameterizations, but run for elevated atmospheric CO_2, **b** ambient model parameterizations with CO_2 fixation capacity (V_{cmax}) and biochemical pools fit for elevated CO_2 plants, **c** elevated CO_2 model parameterizations with all parameters fit for elevated CO_2 plants. **d** Enhancement ratios measured in 1998 (*left*) and 1999 (*right*) under steady-state and light saturating conditions. All three panels of measured enhancement ratios show the same data but are repeated next to each of the model scenarios for ease of comparison

m^{-2}, the ratio of sunfleck:total daily photosynthesis calculated for each model run approached 200% (Fig. 4). Ratios greater than 100% are possible if a large fraction of the diffuse PFD lies below the photosynthetic light compensation point such that without sunflecks A_{day} would be negative. This was common but not universal for sites where PFD <2 mol m^{-2} day^{-1}, or <4% of PFD received above the canopy. For daily PFD>4 mol m^{-2} day^{-1}, the importance of daily sunfleck photosynthesis was much less variable, and the ratio leveled off between 80–90% (Fig. 4). At these sites daily diffuse PFD was always above the species' light compensation points reducing the importance of sunflecks to maintaining a positive day-time C balance.

Under these conditions, limitations to sunfleck photosynthesis at ambient CO_2 decreased in all species with increasing daily PFD. At the lowest daily PFD, dynamic sunfleck photosynthesis for all species modeled can be as low as 50–70% of the steady-state daily prediction (Fig. 5a). For A_{day}, the differences were even larger, with *A. rubrum* showing reductions in A_{day} due to its dynamic behavior of up to 80% (Fig. 5b). At higher daily PFD, when sunflecks are more abundant and of longer duration, the ratios between the dynamic and steady-state models approach 100% for both sunfleck and daily photosynthesis (Fig. 5). Thus, at these higher PFD, limitations to sunfleck photosynthesis become negligible for all species (see also Fig. 3). *L. tulipifera* showed consistently higher ratios of steady-state:dynamic A_{day} than the other species (Fig. 5), suggesting smaller limitations to sunfleck photosynthesis. This resulted in significantly higher A_{day} for *L tulipifera* at low daily PFD (Table 3). At high PFD, when limitations to sunfleck photosynthesis are small, *C. florida* had significantly lower A_{day} than the other species. This was not due to differences in dynamic photosynthesis behavior by *C. florida* but rather due to lower light-saturated A_{net} in comparison to the other species (Table 2).

Table 3 Dynamic model predictions of daily photosynthesis (A_{day}, μmol m^{-2} s^{-1}) under low and moderate daily PFD, and description of the light environments used to run the simulations. Values are means±1 SEM. Repeated measures analysis of variance on A_{day} showed a highly significant species×CO_2 scenario×PFD interaction ($P<<0.01$). *Different letters within each column and ambient/elevated CO_2 scenario* indicate significantly different rates of A_{day} for that species relative to the others ($P<0.05$, Tukey's test). *Scenario a* Ambient model parameterizations, but run for elevated atmospheric CO_2, *scenario b* ambient model parameterizations but CO_2 fixation capacity (V_{cmax}) and biochemical pools fit for elevated CO_2 plants, *scenario c* elevated CO_2 model parameterizations where all parameters were fit for elevated CO_2 plants

	Low daily PFD (1-2 mol m^{-2} day^{-1})	Moderate daily PFD (7–9 mol m^{-2} day^{-1})
PFD (mol m^{-2} day^{-1})	1.62 (0.07)	7.98 (0.66)
% Of above-canopy PFD	2.90 (0.03)	14.50 (1.20)
Sunfleck PFD (mol m^{-2} day^{-1})	0.96 (0.10)	7.20 (0.63)
% Sunfleck PFD	57.69 (4.41)	90.16 (0.52)
n	15	3
Ambient CO_2 predictions		
A. rubrum	10.75 (1.31) [b]	68.82 (1.51) [a]
C. florida	11.11 (1.47) [b]	59.34 (1.76) [b]
L. styraciflua	9.58 (1.15) [b]	66.68 (2.15) [a]
L. tulipifera	13.55 (1.38) [a]	67.98 (1.84) [a]
Elevated CO_2 predictions: scenario [a]		
A. rubrum	18.00 (1.52) [b]	99.73 (2.17) [a]
C. florida	18.22 (1.68) [b]	85.42 (2.50) [c]
L. styraciflua	16.01 (1.33) [b]	94.95 (2.78) [b]
L. tulipifera	20.87 (1.59) [a]	96.28 (2.58) [b]
Elevated CO_2 predictions: scenario [b]		
A. rubrum	19.02 (1.54) [b]	106.07 (2.18) [a]
C. florida	22.64 (1.79) [a]	108.56 (3.08) [a]
L. styraciflua	16.86 (1.36) [c]	100.64 (2.87) [b]
L. tulipifera	18.84 (1.55) [bc]	86.24 (2.36) [c]
Elevated CO_2 predictions: scenario [c]		
A. rubrum	23.64 (1.98) [b]	112.86 (2.63) [a]
C. florida	24.53 (1.92) [a]	111.61 (2.82) [a]
L. styraciflua	19.13 (1.77) [c]	108.81 (2.89) [b]
L. tulipifera	15.50 (1.71) [d]	82.27 (2.27) [c]

A_{day} *in elevated* CO_2

To gain an understanding of how elevated CO_2 would affect A_{day}, we calculated the photosynthetic enhancement ratio (elevated A_{day}/ambient A_{day}). Photosynthesis of the study species was enhanced but not by a constant factor under high and low daily PFD (Fig. 6). This was true for all three versions of elevated CO_2 parameterizations. Ambient parameterizations run at elevated CO_2 – scenario a – had the smallest enhancement ratios at low PFD of the three elevated CO_2 parameterizations used (Fig. 6a). At moderate PFD, this version also predicted a nearly identical enhancement for the four species. This enhancement deviated for some species from the light saturated A_{net} enhancement measured over 2 years (Fig. 6d). Using values for V_{cmax} measured in 1998 for elevated CO_2 in the ambient model parameterization – scenario b – showed higher enhancement ratios at low PFD and, at moderate PFD, resulted in ratios that better matched the measured ones (Fig. 6b). Under this scenario, *L. tulipifera*, the species with the lowest measured photosynthetic enhancement, also showed the lowest enhancement under low PFD. Finally, the elevated CO_2 parameterizations – scenario c – showed further increases in low PFD enhancement ratios over the ambient CO_2 parameterizations for three of the species. *L. tulipifera*, however, had the lowest enhancement ratios of the species, and enhancement was independent of daily PFD (Fig. 6c). At moderate PFD, enhancement ratios were again similar to those measured.

As a result of the predicted enhancements, all species had significantly higher A_{day} under elevated CO_2 (Table 3). Using the ambient models run at elevated CO_2 yielded the same species differences as under ambient CO_2: relative to the other species, *L. tulipifera* had significantly higher A_{day} under low PFD, and *C. florida* had significantly lower A_{day} under high PFD. However, using ambient parameterizations with elevated CO_2 V_{cmax} or elevated CO_2 parameterizations (scenarios b and c), *L. tulipifera* lost its photosynthetic advantage at low PFD and had significantly lower A_{day} at moderate PFD than the other species (Table 3). At moderate PFD, this was the result of lower photosynthetic enhancement for *L. tulipifera* that was incorporated into the model parameterization (Fig. 6). These three scenarios show that if elevated CO_2 plants do not change their carboxylation capacity and biochemical pools, A_{day} enhancements can be inferred with reasonable accuracy from those measured under light saturated conditions. If however adjustments in either biochemistry or dynamic behavior occur, then A_{day} enhancement can differ substantially from measured enhancements at low daily PFD.

Discussion

It is not surprising that species' differences in dynamic behavior can have a potentially significant impact on daily sunfleck and total photosynthesis under low daily PFD conditions (Fig. 5, Table 3), but few studies have

been able to separate the effects of light environment from those of species-specific dynamic responses (Pearcy et al. 1994). This is in spite of the recognition that dynamic photosynthetic responses to light can impact A_{day} (Chazdon 1988; Pearcy 1990). Using a modeling approach, we were able to show the consequences of observed species differences in dynamic behavior on daily leaf-level C uptake on a sunny day (Fig. 5, Table 3). Our initial prediction was that the most asymmetrical sunfleck behavior, fast stomatal and photosynthetic enzyme induction, and slow loss of induction, would maximize A_{day} in different sunfleck regimes. Under low daily PFD, this hypothesis was supported by results for *L. tulipifera*, which indeed had the highest A_{day} of the species. However, under moderate light levels differences in dynamic sunfleck behavior had minimal effects on A_{day} (Fig. 5, Table 3).

At the moderate daily PFD levels characteristic of more open understory microsites, sunflecks would be frequent and long, and high PFD could be maintained for up to an hour (data not shown). Under these conditions, species differences in dynamic photosynthesis become less important to overall A_{day} than under low PFD conditions (Fig. 5) and hence light-saturated A_{net} has a greater impact on A_{day}. With a lower light-saturated A_{net} for *C. florida* (Table 2), A_{day} in this species was also significantly lower than in the other species. Thus, in environments with moderate to high understory PFD that have long periods of direct PFD, modeling approaches utilizing steady-state measures are likely adequate for estimating A_{day} (Figs. 3, 5; Pearcy et al. 1994; Naumburg and Ellsworth to be published).

A_{day} estimates in this study were based on predictions by a dynamic photosynthesis model that has been shown to reproduce dynamic sunfleck responses well in other species (Pearcy et al. 1997; Kirschbaum et al 1998). Our goal in this study was to compare species A_{day}, thus, we parameterized the model for a population rather than individuals by using parameters that describe the "average" response to variable PFD of a species and CO_2 treatment. As such, we could not test the model against A_{net} measurements specific to the plant from which the model parameters were derived as in previous studies (Pearcy et al. 1997; Kirschbaum et al. 1998), and as a result model performance can expected to be worse than in these previous studies. Instead, we used daily courses of A_{net} of individual plants measured in an forest understory under ambient environmental conditions for comparing model outputs against measurements. RMSE analysis of the measured and modeled A_{net} showed that incorporating dynamic PFD responses is important when the time interval of interest is short, and over longer time intervals for species highly responsive to variable light (Fig. 2). Thus, despite expectations that the model would deviate from measured A_{net} due to using population parameters and testing them against individual leaf A_{net}, the dynamic model was superior under most circumstances. Given that the dynamic and steady-state parameterizations for *L. tulipifera* result in comparatively small differences in A_{net} and A_{day} predictions (e.g., Fig. 5), it is also expected that the difference RMSE for this species are small irrespective of the time scale (Fig. 2). However, even for species with large limitations to sunfleck photosynthesis the performance difference between the model types decayed with increasing time scales. Again, this may be an artifact of the model testing employed in this study where it is expected that both model types err in their A_{net} predictions. By increasing the time scale over which that data was averaged, the errors of both dynamic and steady-state models would average out and thus the difference between the accuracy of the two model predictions would decrease. However, since the dynamic model predicted A_{net} better at the short time scales where sunfleck dynamics generally operate (Pearcy et al. 1994) and the potentially large differences in daily predictions of photosynthesis between the model types (up to 40%, Naumburg and Ellsworth to be published), we would advocate the use of dynamic models even over longer time scales under low daily PFD environments where dynamic responses likely affect A_{day}.

Using the dynamic model, we further investigated the effect of a 20.0 Pa increase of CO_2 on A_{day} under three different scenarios: (1) no acclimation to CO_2 (Fig. 6a), (2) carboxylation capacity and biochemical pools (e.g., V_{cmax}, V_{Jmax}, V_{Fmax}, R_{max} and T_{max}) are altered under elevated CO_2 (Fig. 6b), and (3) complete elevated CO_2 parameterization (Fig. 6c). Under all three scenarios, photosynthetic enhancements at low daily PFD were larger than at moderate PFD or during measurements of light-saturated A_{net}. Consequently, rising CO_2 may benefit plants growing in poor light microsites relatively more than at better microsites (Bazzaz and Miao 1993; Osborne et al. 1997; Würth et al. 1998), and this benefit cannot be inferred from light-saturated A_{net} measurements alone.

Additionally, stomatal responses to elevated CO_2, both steady state and dynamic, could influence A_{day}. These factors were not incorporated here since they were not observed for the study species under well-watered (Naumburg and Ellsworth 2000) and drought conditions (E. Naumburg, unpublished data). Further, in their meta-analysis of 48 recent, elevated-CO_2 studies on woody species, Curtis and Wang (1998) found only a modest and non-significant reduction of 11% in response to elevated CO_2. Given the high variability in understory light environments and the relatively infrequent times in the day when maximum A_{net} and stomatal conductance are achieved, stomatal responses to elevated CO_2 in understory trees are unlikely to strongly affect daily A_{net} in the absence of large effects on stomatal conductance and its response dynamics.

With respect to the different species studied, both the degree of photosynthetic enhancement and predicted A_{day} varied with the three scenarios. Predictably, assuming no adjustments under elevated CO_2 (scenario a) yields similar enhancements (Fig. 6a) and thus the same ranking for the species' A_{day} as under ambient CO_2 (Table 3). However, if either biochemical kinetics or overall dynamic

behavior change under elevated CO_2, then the outcomes can differ. Under both of these scenarios (b and c), *L. tulipifera* had lower A_{day} enhancement than the other species (Fig. 6b, c) and no longer had the highest elevated CO_2 A_{day}. Indeed, the model results predict that the two shade-tolerant species, *C. florida* and *A. rubrum*, would see the greatest benefit from elevated CO_2 under low PFD (Table 3). These predictions agree with findings that shade-tolerant species tend to have greater photosynthetic and growth enhancements under elevated CO_2 than shade-intolerant species (Kerstiens 1998; Hättenschwiler and Körner 2000).

Our predictions of A_{day} under ambient CO_2 raise the question of why *L. tulipifera*, the least shade tolerant of the species we studied, would have the highest A_{day}. This species typically shows high understory mortality in the absence of forest gaps (Baker 1949; Burns and Honkala 1990), and will never reach maturity in typical understory shade conditions. There are three major reasons why higher leaf-level C uptake may not directly translate into higher growth or survival. First, the models were parameterized from data collected early in the growing season under ideal environmental conditions and run on PFD data from a sunny day. However, in North Carolina summer days are often partly cloudy and under these conditions sunflecks are less frequent and therefore become less important to A_{day}. Thus, our model predictions should be viewed as upper-limit estimates of A_{day}. Second, drought can be common in southeastern forests and conditions may not be as favorable during the growing season as they were during parameterization measurements. *L. tulipifera* responds to reductions in soil water potential with greater stomatal closure than *A. rubrum* and *L. styraciflua* (Roberts et al. 1979; Croker et al. 1998; Pataki 1998) and early, partial leaf senescence (Burns and Honkala 1990; E. Naumburg, personal observation). Thus, environmental factors not explicitly considered in this study could differentially affect the competing species in our study and reduce the seasonal C balance of sensitive species such as *L. tulipifera*.

Third, leaf-level C uptake is only one component of whole-plant C balance (Körner 1991; Lambers and Poorter 1992; Walters et al. 1993; Walters and Reich 1996, 1999). Plant allometry such as allocation to leaves or the leaf area ratio (ratio of plant leaf area to total biomass) together with whole-plant respiration can have a large impact on growth and survival under low light (Walters et al. 1993; Walters and Reich 1996; Kitajima 1994; Huante and Rincon 1998; Naumburg et al. to be published). Shade-tolerant and intolerant species tend to differ in these characteristics with shade-intolerant species generally having higher allocation to leaves and higher leaf area ratios (Veneklaas and Poorter 1998; Walters and Reich 1999). These traits would contribute to higher growth potentials in shade-intolerant species in moderate to high light environments, but also to higher whole plant respiration (Walters and Reich 1996, 1999; Poorter and Lambers 1992). Shade-intolerant plants may preferentially allocate more C to growth than storage and thus increase the chance of adverse events that decrease C uptake (e.g., defoliation, drought) leading to mortality (Walters and Reich 1999). Indeed, many shade-intolerant species show lower survivorship than tolerant species for a given rate of stem growth (Kobe et al. 1995; Kobe and Coates 1997). Thus, despite an advantage in leaf-level daily C uptake by *L. tulipifera* compared to co-occurring species, this alone may not necessarily lead to greater survival or a successional advantage over the other species. In fact, *L. tulipifera* is the only one of the four hardwood species studied in which we have observed sapling mortality in the three years since the start of the FACTS-1 experiment (E. Naumburg, unpublished data).

The species in our study have only shown small photosynthetic adjustments in their photosynthetic capacity and dynamic responses to elevated CO_2 (Naumburg and Ellsworth 2000; DeLucia and Thomas 2000) unlike tree seedlings and saplings in many other studies (Gunderson and Wullschleger 1994; Saxe et al. 1998; Curtis 1996). Because of this, A_{day} photosynthetic enhancement ratios for three of the four species were in the range of 2 or greater. Having such large enhancement ratios could be crucial for plants to survive in these low PFD environments irrespective of their allometry, since low A_{day} during sunny days could easily be zero or negative for days when understory radiation is reduced due to weather conditions and overstory leaf area dynamics. Consequently, even small photosynthetic adjustments under elevated CO_2 could have profound impacts on individual species' performance in marginal understory sites because these differences do not only compound on a daily but also on a seasonal basis.

Acknowledgements We would like to thank J. Edeburn of Duke Forest and A. Palmiotti, K. Lewin, J. Nagy, and G. Hendrey of B. N. L. for maintaining the site facilities. We further thank M. Walters, R. Oren, an anonymous reviewer who made valuable comments on earlier versions of the manuscript. This research is part of the Forest-Atmosphere Carbon Transfer and Storage (FACTS-1) project at Duke University. The FACTS-1 project is supported by the U.S. Department of Energy, Office of Biological and Environmental Research, under DOE contract DE-AC02-98CH10886 at Brookhaven National Laboratory and contract DE-FG05-95ER62083 at Duke University.

Appendix I

We employed the dynamic model of photosynthesis of Pearcy et al. (1997) in our understory tree photosynthesis simulations. The model is a modification of the commonly used Farquhar photosynthesis model formulation (Farquhar and von Caemmerer 1982) and includes parameters representing light-induced activation and deactivation of key photosynthetic enzymes, and metabolite pools that mediate stomatal dynamics during sunflecks. The model consists of two major modules (stomatal and biochemical) described below. The stomatal module computes the light-mediated stomatal conductance to water vapor (g_w) which is used to predict leaf internal CO_2 concentration (c_i) in an iterative fashion using the stomatal conductance to CO_2 (g_c) calculated from g_w along with outputs from the biochemical model. The variables and symbols used here are defined in Table 1. Each of the differential equations in the model was solved using the 4th order Runge-Kutta method.

Stomatal module

For each PFD input value, the model calculates the equilibrium stomatal conductance to water vapor ($g_{w\,eq}$) first:

$$g_{w\,eq} = \frac{\alpha_g \times PFD + g_{w\,sat} - \left[(\alpha_g \times PDF + g_{w\,sat})^2 - 4 \times \theta_g \times \alpha_g \times g_{w\,sat} \times PDF\right]^{0.5}}{2 \times \theta_g} 2 \quad (1)$$

where $g_{w\,sat}$ is light-saturated stomatal conductance to water vapor, α_g is the initial slope of g_w light response, θ_g is a curvature parameter.

Dynamic stomatal responses to changes in PFD are then modeled using three equations by mimicking processes in the guard cells. The first equation is based on a biochemical signal (b) that triggers stomatal opening and closing. The second equation represents the subsequent influx/efflux of osmotica (k) in guard cells and the third the movement of water (w) into and out of the guard cells. The equations generate relative values ranging between 0 and 1. Depending on whether $g_{w\,eq}/g_{w\,sat}$ is smaller or larger than the biochemical signal value calculated in the previous time step [$b_{(t-1)}$], either the equation for a increase or decrease of b is used:

$$b_{(t)} = \frac{\frac{g_{weq}}{g_{sat}} - b_{(t-1)}}{\tau_{gi}} \quad (2)$$

or

$$b_{(t)} = \frac{\frac{g_{weq}}{g_{sat}} - b_{(t-1)}}{\tau_{gd}} \quad (3)$$

where τ_{gi} is a time constant for a biochemical opening signal and τ_{gd} is a time constant for a biochemical closing signal. This value of the biochemical signal is then used in the osmotica equation:

$$k_{(t)} = \frac{b_{(t)} - k_{(t-1)}}{\tau_{gk}} \quad (4)$$

where τ_{gk} is a time constant for osmotica in-/efflux. The value for osmotica is in turn used in the water equation:

$$w_{(t)} = \frac{k_{(t)} - w_{(t-1)}}{\tau_{gw}} \quad (5)$$

where τ_{gw} is a time constant for water in-/efflux.

Finally, $w_{(t)}$ directly translates into stomatal conductance to water vapor via:

$$g_{w(t)} = w_{(t)} \times g_{w\,sat} \quad (6)$$

which is used along with A_{net} output by the biochemical module to predict c_i.

Biochemical module

Equilibrium values of variables V_c, V_f, and V_j are calculated for the input light value using a non-rectangular hyperbola similar to Eq. 1. V_j is assumed to be responding instantaneously to changes in PFD whereas V_c and V_f have time constants for activation and deactivation associated with them. Values of V_c and V_f for the current time step t are calculated equivalently to the stomatal parameters (see Eqs. 2, 3). Using these parameters and the c_i of the previous time step (t–1), an approximate value of W_c, the ribulose-bisphosphate-saturated rate of carboxylation, and approximate values of the pool sizes of T, R, and G are calculated:

$$W_c = \frac{V_c \times c_i^2}{(c_i + K_a) \times \{c_i + K_c \times (1 + [O_2]/K_O\}} \quad (7)$$

where [O_2] is the pressure of O_2 (21,000 Pa)

$$T_{(t)} = V_j \times \left[1 - \frac{T_{(t-1)}}{T_{(max)}}\right] - \frac{5}{3} \times \frac{V_{f(t)} \times T_{(t-1)}}{K_T + T_{(t-1)}} \times \left[1 - \frac{R_{(t-1)}}{R_{max}}\right] \quad (8)$$

$$R_{(t)} = \frac{V_{f(t)} \times T_{(t-1)}}{K_T + T_{(t-1)}} \times \left(1 - \frac{R_{(t-1)}}{R_{max}}\right) - \left(1 + \frac{2 \times \Gamma^*}{c_i}\right) \times W_c \times \frac{R_{(t-1)}}{K_R + R_{(t-1)}} \quad (9)$$

where Γ^* is CO_2 compensation in the absence of photorespiration.

$$G_{(t)} = \frac{2 \times \Gamma^*}{c_i} \times W_c \times \frac{R_{(t-1)}}{K_R + R_{(t-1)}} - \Psi \times G_{(t-1)} \quad (10)$$

Using these values, a first approximation of A_{net} during the current time step can be calculated:

$$A_{net} = W_c \times \frac{R_{(t)}}{R_{(t)} + K_R} - 0.5 \times \Psi \times G_{(t)} - R_d \quad (11)$$

A_{net} can also be calculated using the Fick's law equation:

$$A_{net} = \frac{c_a - c_i}{P_{atm}} \times g_c \quad (12)$$

which uses g_c, the stomatal conductance to CO_2 input by the stomatal module, and atmospheric pressure, P_{atm}. Substituting Eq. 7 into Eq. 11 and setting Eqs. 11 and 12 equal yields the following:

$$Y = -0.5 \times \Psi \times G_{(t)} - R_d + \frac{V_c \times c_i^2}{(c_i + K_a) \times \{c_i + K_c \times (1 + [O_2]/K_O)\}} \times \frac{R_{(t)}}{R_{(t)} + K_R} - g_c \times \frac{c_a - c_i}{P_{atm}} \quad (13)$$

where Y should be zero. Given the current values for R and G, the program iteratively finds a c_i that meets this criterion. This newly estimated c_i is then used to determine new values for W_c, T, R, and G using Eqs. 7–10 for the current time step. This loop is repeated until the solutions of Eqs. 11 and 12 converge.

For the steady-state photosynthesis model, the dynamic model above is used where time constants (τ) are set to zero, and only Eq. 12 is solved for c_i. Again, this intermediary c_i was used to recalculate W_c, T, R, and G. We chose this solution because unlike the dynamic model c_i can jump dramatically with each new PFD reading so that using Eq. 13 is too computationally demanding. Both methods provided stable solutions.

References

Baker FS (1949) A revised tolerance table. J For 47:179–181

Bazzaz FA, Miao SL (1993) Successional status, seed size, and responses of tree seedlings to CO_2, light, and nutrients. Ecology 74:104–112

Bolker BM, Pacala SW, Bazzaz FA, Canham CD, Levin SA (1995) Species diversity and ecosystem response to carbon dioxide fertilization: conclusions from a temperate forest model. Global Change Biol 1:373–381

Burns RM, Honkala BH (1990) Silvics of North America. II. Hardwoods. USDA Agriculture Handbook no. 654. USDA, Washington D.C.

Chazdon RL (1988) Sunflecks and their importance to forest understorey plants. Adv Ecol Res 18:1–63

Croker JL, Witte WT, Auge RM (1998) Stomatal sensitivity of six temperate, deciduous tree species to non-hydraulic root-to-shoot signaling of partial soil drying. J Exp Bot 49:761–774

Curtis PS (1996) A meta-analysis of leaf gas exchange and nitrogen in trees grown under elevated carbon dioxide. Plant Cell Environ 19:127–137

Curtis PS, Wang X (1998) A meta-analysis of elevated CO_2 effects on woody plant mass, form and physiology. Oecologia 113: 299–313

DeLucia EH, Thomas RB (2000) Photosynthetic responses to CO_2 enrichment of four hardwood species in a forest understory. Oecologia 122:11–19

Farquhar GD, Caemmerer S von (1982) Modelling of photosynthetic response to environmental conditions. In: Lange OL, Nobel PS, Osmond CB, Ziegler H (eds) Physiological plant

ecology. II. Water relations and carbon assimilation. Springer, Berlin Heidelberg New York, pp 549–587
Gross LJ (1982) Photosynthetic dynamics in varying light environments: a model and its application to whole leaf carbon gain. Ecology 63:84–93
Gunderson CA, Wullschleger SD (1994) Photosynthetic acclimation in trees to rising atmospheric CO_2: a broader perspective. Photosynth Res 39:369–388
Hättenschwiler S, Körner C (2000) Tree seedling responses to in situ CO_2-enrichment differ among species and depend on understorey light availability. Global Change Biol 6:213–226
Hendrey GR, Ellsworth DS, Lewin KF, Nagy J (1999) A free-air enrichment system for exposing tall forest vegetation to elevated atmospheric CO_2. Global Change Biol 5:293–309
Huante P, Rincon E (1998) Responses to light changes in tropical deciduous woody seedlings with contrasting growth rates. Oecologia 113:53–66
Kerstiens G (1998) Shade-tolerance as a predictor of responses to elevated CO_2 in trees. Physiol Plant 102:472–480
Kirschbaum MUF, Gross LJ, Pearcy RW (1988) Observed and modelled stomatal responses to dynamic light environments in the shade plant *Alocasia macrorrhiza*. Plant Cell Environ 11: 111–121
Kirschbaum MUF, Küppers M, Schneider HGC, Noe S (1998) Modelling photosynthesis in fluctuating light with inclusion of stomatal conductance, biochemical activation and pools of key photosynthetic intermediates. Planta 204:16–26
Kitajima K (1994) Relative importance of photosynthetic traits and allocation patterns as correlates of seedling shade tolerance of 13 tropical trees. Oecologia 98:419–428
Kobe RK, Coates KD (1997) Models of sapling mortality as a function of growth to characterize interspecific variation in shade tolerance of eight tree species of northwestern British Columbia. Can J For Res 27:227–236
Kobe RK, Pacala SW, Silander JA Jr (1995) Juvenile tree survivorship as a component of shade tolerance. Ecol Applic 5: 517–532
Körner C (1991) Some often overlooked plant characteristics as determinants of plant growth: a reconsideration. Funct Ecol 5: 162–173
Lambers H, Poorter H (1992) Inherent variation in growth rate between higher plants: a search for physiological causes and ecological consequences. Adv Ecol Res 23:187–261
Leuning R (1995) A critical appraisal of a combined stomatal-photosynthesis model for C_3 plants. Plant Cell Environ 18: 339–357
Naumburg E, Ellsworth DS (2000) Photosynthetic sunfleck utilization potential of understory saplings growing under elevated CO_2. Oecologia 122:163–174
Osborne CP, Drake BG, LaRoche J, Long SP (1997) Does long-term elevation of CO_2 concentration increase photosynthesis in forest floor vegetation? Plant Physiol 114:337–344
Pataki DE (1998) Water use of co-occurring species in response to environmental conditions at varying temporal scales. PhD dissertation. Duke University, N.C.
Pearcy RW (1987) Photosynthetic gas exchange responses of Australian tropical forest trees in canopy, gap and understory micro-environments. Funct Ecol 1:169–178
Pearcy RW (1990) Sunflecks and photosynthesis in plant canopies. Annu Rev Plant Physiol Plant Mol Biol 41:421–453
Pearcy RW, Calkin HW (1983) Carbon dioxide exchange of C_3 and C_4 tree species in the understory of a Hawaiian forest. Oecologia 58:26–32
Pearcy RW, Pfitsch WA (1991) Influence of sunflecks on the $\delta^{13}C$ of *Adenocaulon bicolor* plants occurring in contrasting forest understory microsites. Oecologia 86:457–462
Pearcy RW, Chazdon RL, Gross LJ, Mott KA (1994) Photosynthetic utilization of sunflecks: a temporally patchy resource on a time scale of seconds to minutes. In: Caldwell MM, Pearcy RW (eds) Exploitation of environmental heterogeneity by plants. Academic Press, San Diego, Calif., pp 175–208
Pearcy RW, Krall JP, Sassenrath-Cole GF (1996) Photosynthesis in fluctuating light environments. In: Baker NR (ed) Photosynthesis and the environment. Kluwer, Dordrecht, pp 321–346
Pearcy RW, Gross LJ, He D (1997) An improved dynamic model of photosynthesis for estimation of carbon gain in sunfleck light regimes. Plant Cell Environ 20:411–424
Pfitsch WA, Pearcy RW (1989) Daily carbon gain by *Adenocaulon bicolor*, a redwood forest understory herb, in relation to its light environment. Oecologia 80:465–470
Poorters and Lambers (1992) Inherent variation in growth rate between higher plants: a search for physiological causes and ecological consequences. Adv Ecol Res 23:187-261
Roberts SW, Knoerr KR, Strain BR (1979) Comparative field water relations of four co-occurring forest tree species. Can J Bot 57:1876–1882
Sassenrath-Cole GF, Pearcy RW (1994) Regulation of photosynthetic induction state by the magnitude and duration of low light exposure. Plant Physiol 105:1115–1123
Saxe H, Ellsworth DS, Heath J (1998) Tree and forest functioning in an enriched CO_2 atmosphere. New Phytol 139:395–436
Sims DA, Pearcy RW (1993) Sunfleck frequency and duration affects growth rate of the understorey plant, *Alocasia macrorrhiza*. Funct Ecol 7:683–689
Valladares F, Allen MT, Pearcy RW (1997) Photosynthetic response to dynamic light under field conditions in six tropical rainforest shrubs occurring along a light gradient. Oecologia 111:505–514
Veneklaas EL, Poorter L (1998) Growth and carbon partitioning of tropical tree seedlings in contrasting light environments. In: Lambers H, Poorter L, Vuurren MMI van (eds) Inherent variation in plant growth: physiological mechanisms and ecological consequences. Backhuys, Leiden, pp 337–362
Walters MB, Reich PB (1996) Are shade tolerance, survival, and growth rate linked? Low light and nitrogen effects on hardwood seedlings. Ecology 77:841–853
Walters MB, Reich PB (1999) Low-light carbon balance and shade tolerance in the seedlings of woody plants: do winter deciduous and broad-leaved evergreen species differ? New Phytol 143:143–154
Walters MB, Kruger EL, Reich PB (1993) Relative growth rate in relation to physiological and morphological traits for northern hardwood tree seedlings: species, light environment and ontogenetic considerations. Oecologia 96:219–231
Watling JR, Ball MC, Woodrow IE (1997) The utilization of light-flecks for growth in four Australian rain-forest species. Funct Ecol 11:231–239
Wayne PM, Bazzaz FA (1993) Birch seedling responses to daily time courses of light in experimental forest gaps and shadehouses. Ecology 74:1500–1515
Würth WKR, Winter K, Körner C (1998) In situ responses to elevated CO_2 in tropical forest understorey plants. Funct Ecol 12:886–895